

COMPARISON BETWEEN DIFFERENT FLUX TRAPS ASSEMBLED IN THE CORE OF THE NUCLEAR REACTOR IPEN/MB-01 BY MEASURING OF THE THERMAL AND EPITHERMAL NEUTRON FLUXES USING ACTIVATION FOILS

**Luiz Ernesto Credidio Mura , Ulysses d'Utra Bitelli ,
Luis Felipe Liambos Mura, Thiago Carluccio, Graciete Simões de Andrade**

Instituto de Pesquisas Energéticas e Nucleares (IPEN / CNEN - SP)

Av. Professor Lineu Prestes 2242

05508-000 São Paulo, SP

credidiomura@gmail.br

ubitelli@ipen.br

lflmura@gmail.com

thiagocarluccio@gmail.com

gsasilva@ipen.br

ABSTRACT

The production of radioisotopes is one of the most important applications of nuclear research reactors. This study investigated a method called Flux Trap, which is used to increase the yield of production of radioisotopes in nuclear reactors. The method consists in the rearrangement of the fuel rods to allow the increase of the thermal neutron flux in the irradiation region inside the reactor core, without changing the standard reactor power level. Various configurations were assembled with the objective of finding the configuration with the highest thermal neutron flux in the region of irradiation. The method of activation analysis was used to measure the thermal neutron flux and determine the most efficient reactor core configuration. It was found that there was an increase in the thermal neutron flux of 337% in the most efficient configuration, which demonstrates the effectiveness of the method.

1. INTRODUCTION

Global demand for radioisotopes is growing faster than production, which has generated interest in methods to increase production yields of these elements in nuclear research reactors. This study aims to analyze the Flux Trap method that generates an increase in the thermal neutron flux in the region of radiation without the need for change in the standard reactor power level [1]. The assembly of a Flux Trap in a thermal nuclear reactor moderated by water consists of removing fuel rods from a particular region of the reactor

core. Thus, the Flux Trap is a region of the reactor core filled only by the moderator. The neutrons that penetrate the Flux Trap collide only with water molecules. The fast neutrons generated by nuclear fissions in the fuel rods enter these regions and are thermalized by elastic scattering nuclear reactions with water molecules (hydrogen atoms) generating the increase of thermal neutron flux inside the Neutron Flux Trap. The Fig. 1 is a schematic of a Neutron Flux Trap assembled in the reactor core IPEN/MB-01. In this Flux Trap assembly, the standard rectangular core configuration was changed by removing fuel rods from the center of the core.

This work assembled several core configurations with different geometries of Neutrons Flux Traps. Due to loss of reactivity caused by the removing of the fuel rods from the center of the core some Neutron Flux Traps do not reach criticality level. The measurements of the thermal neutron flux at the center of the nuclear core configuration number 203 show the most efficient configuration of Neutron Flux Trap, because in this configuration highest thermal neutron flux and cadmium ratio values are obtained when compared with other Neutron Flux Traps in the same central position core. These Neutron Flux Trap assemblies are always compared with the standard rectangular core configuration compounds by 28x26 fuel rods. The position of comparison of the thermal neutron fluxes is the center of the reactor core, which is the same position of the center of Flux Trap. Measurements of neutron fluxes of the standard configuration had already been made [2] and were normalized with the same operating reactor power level. The most efficient Neutron Flux Trap number 203 (FT 6X6 and Octagonal fuel rods external shape) shows an increase in thermal neutron flux of approximately 337% when compared with the standard configuration core in the same reactor power level, demonstrating the effectiveness of the method.

Activation foils [3,4,5,6,7] are used to obtain the thermal neutron flux inside the Neutron Flux Trap due to accuracy and precision of this absolute method. The spatial distribution of neutrons flux is used to compare the increase of the thermal neutron flux at the center of Flux Trap along of the active region of the fuel reactor core. The discrete cross sections of the library ENDF/B-VII.0 [8] and their corresponding mean values in each energy group weighted by the spectrum calculated by MCNP-4C code [9,10] are used to obtain the effective thermal cross section of the gold foil infinitely diluted with aluminum atoms.

2. EXPERIMENTAL METHODOLOGY

2.1. The Nuclear Reactor IPEN/MB-01

The IPEN/MB-01 nuclear reactor is a zero power reactor with self-limiting power of 100 watts. The reactor is moderated, reflected and shielded by demineralized light water and has a reactor core assembled in a stainless steel plate with 900 holes in a 30x30 array. In its standard configuration 680 fuel rods composed of UO_2 enriched to 4.3% and clad with 304 stainless steel are inserted and it has 24 control rods made of an alloy of Ag-In-Cd set in two control rods. One of the items of the security system allows automatic shutdown of the reactor and is composed of two safety bars with 12 rods each composed of B_4C . The reactor was designed to allow the measurement of parameters for studies of nuclear reactor physics and some of the experiments conducted in the reactor were classified as OECD / NEA (benchmarks). It also allows experiments to be carried out with educational and training purposes.

2.2 Power Reactor Operation

The power reactor level is obtained by the counting rate of the nuclear channel number 10 (^{10}B neutron detector). This nuclear channel is always used because its detector is far enough from the reactor core, thus providing a realistic estimate of the level of power reactor. The nuclear channel number 10 is sensitive to little differences in power level during the irradiations and it is always used to normalize the value of power level.

The value of the power level of 67.89 watts given by the nuclear channel 10 shows good agreement when compared with the value obtained using the methodology of analysis by noise [11] (61.15 ± 8.28 watts [12]).

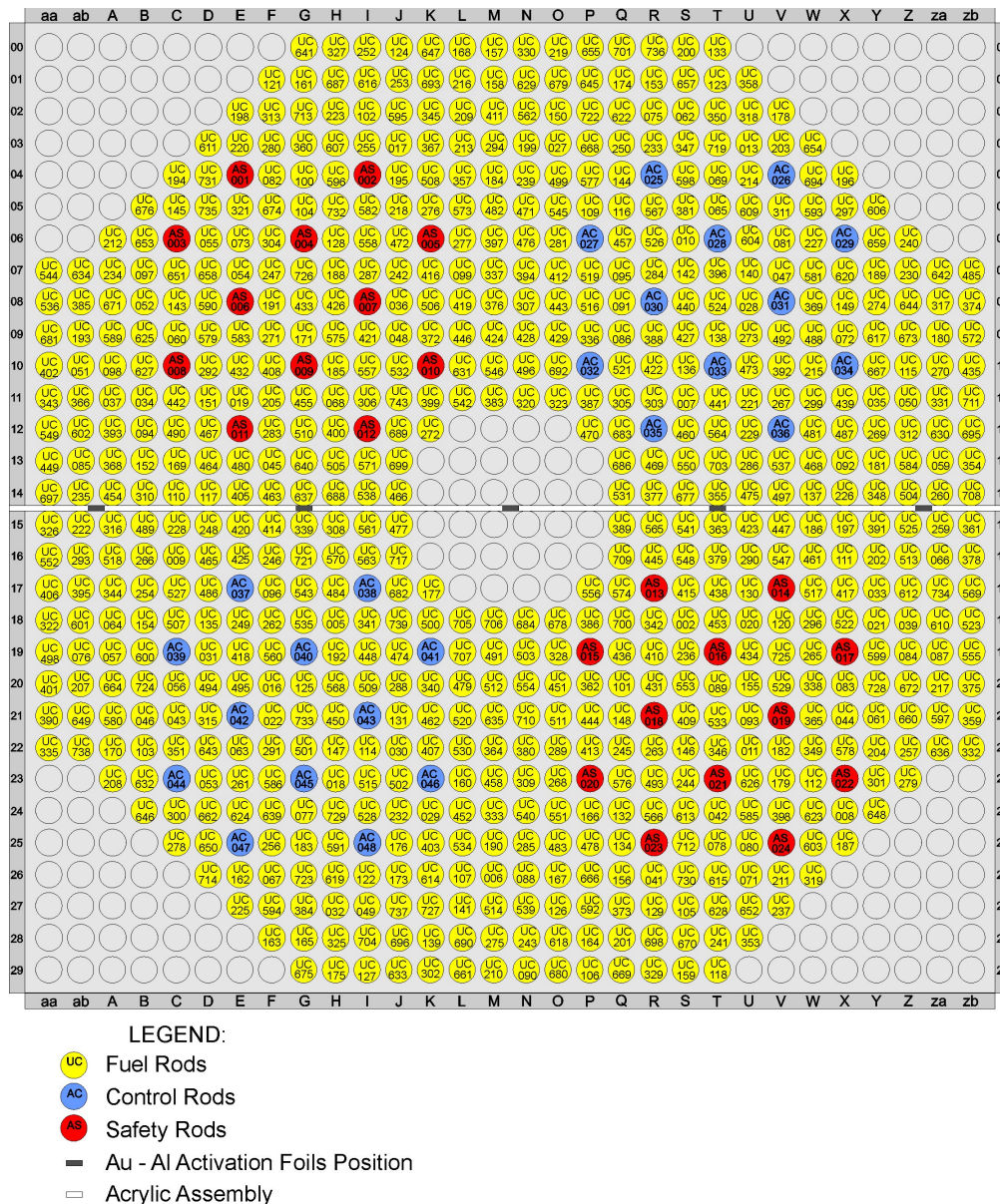


Figure 1. Reactor Core (Configuration N° 203) with Neutron Flux Trap at the center and Au-Al activation Foils at irradiation positions.

2.3 Irradiation of the Activation Foils in The IPEN/MB-01 Reactor Core

This work uses infinitely diluted gold foils as activation detectors to determine the thermal and epithermal neutron flux. These foils are chosen to make negligible the effects of self-shielding avoiding the use of complex correction factors in the calculations of thermal neutron fluxes. These foils are called infinitely diluted because they are composed of an alloy where 1% of the total mass of the alloy is composed by gold (large cross section value to nuclear reaction) diluted in a matrix of aluminum (very small cross section to thermal neutrons).

The dimensions of these foils are 0.02 cm and 0.75 cm of thickness and diameter, respectively. Their distribution is made on an acrylic plate in an arrangement of 5x7. Thus, a total of 11 foils were irradiated as showed in the Fig. 2.

Fig. 2 shows that the first line of the acrylic plate is indicated as 91 mm axial quote and that it corresponds to the beginning of the fuel active region (fuel rod \rightarrow UO₂), and that the last line is indicated as 637 mm axial quote and that it is the end of the active region. The height of the active region is 546 mm and corresponds to the height of the fuel rod.

The positions of 1,2,3,4 and 5 given at Fig. 2 (showed at Fig. 1 and Fig. 3) correspond to 27.750 mm, 125.075 mm, 222.400 mm, 319.725 mm and 417.050 mm radial quotes, respectively. The Activation foils positions are showed in Fig. 1 and Fig. 3.

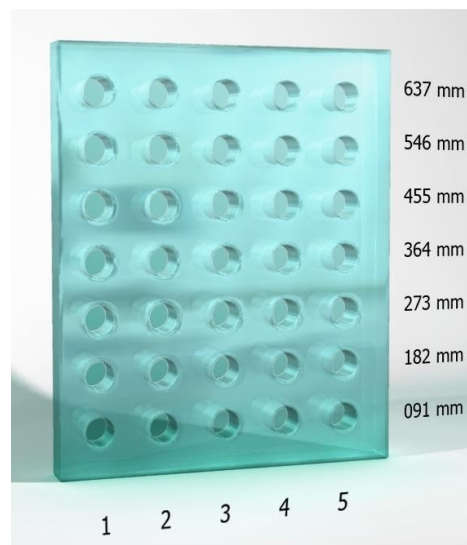


Figure2. Illustration of the acrylic plate and the axial and radial positions of the activation foils.

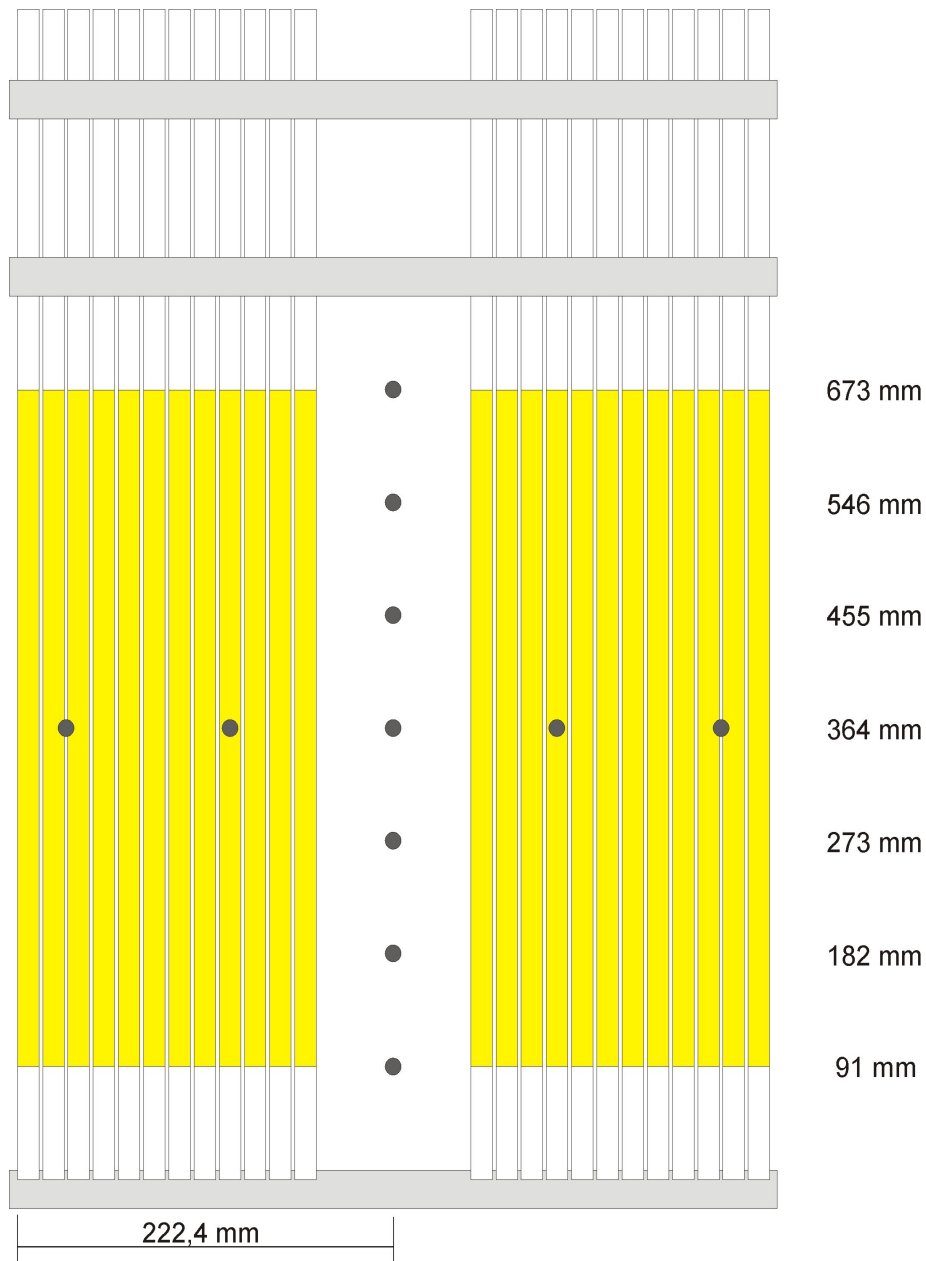


Figure 3. Configuration of the Flux Trap with Activation foils positions along radial and Axial Positions in the IPEN/MB-01 Reactor Core.

Each of the 11 points are mapped, thus are irradiated 22 foils. For each point a bare foil and a foil covered with cadmium of 0.508 mm thickness are irradiated. Thus it is necessary to perform two irradiations in the same operational conditions which have a power level of 67.89 watts (nuclear channel 10) and in the same control rods position. This procedure is adopted to determine the cadmium ratio, R_{cd} , in each irradiation position.

After the irradiations, the foils are analyzed in the detection system of hyper-pure germanium (HPGe) to gamma spectrometry, as showed in the Fig. 4:



Figure 4. The detection system of hyper-pure germanium (HPGe).

With the values of the net gamma counting at 411.80 keV of the ^{198}Au produced through nuclear reaction $^{197}\text{Au}(n,\gamma)^{198}\text{Au}$ for each foil, the next step is to obtain the saturation activity (nuclear reaction rate) by equation (1)

$$A^\infty = \frac{e^{\lambda_e} C}{\varepsilon I L T (1 - e^{-\lambda t_i})} \frac{F_r F_a}{F_n} \quad (1)$$

where λ is the decay constant, t_e is the waiting time to the gamma spectrometry after the irradiation, C is the net counting of the gamma energy, ε is the global efficiency of the system of the gamma spectrometry, I is the branching ratio to the gamma energy, $L T$ is the counting Live Time during the gamma spectrometry, t_i is the irradiation time, F_r is the ramp reactor power level factor, F_n is the factor which considers the little fluctuation in the power level between the irradiations and F_a is the gamma self-absorption factor during the counting foil.

The thermal neutron flux is obtained by equation (2) [13].

$$\varphi_{th} = \frac{A_{Bared} \left(1 - \frac{F_{cd}}{R_{cd}} \right) P_a}{N_a m \sigma_{av}} \quad (2)$$

where P_a is the atomic weight of the target nucleus, N_a is the Avogadro's number, m is the mass of the activation foil, σ_{av} is the microscopic activation cross section, R_{cd} the cadmium ratio and F_{cd} is the factor cadmium (1.054) [2,14].

The epithermal neutron flux can be obtained by Equation (3) [13].

$$\phi_{\text{int}} = \frac{A_{\text{Bared}}^{\infty}}{N_T I_R^{\infty} R_{cd}} \ln \frac{E_2}{E_{cd}} \quad (3)$$

where N_T is the total number of target atoms in the foil, I_R^{∞} is the resonance integral, R_{cd} is the cadmium ratio, E_2 is the energy between intermediate and fast regions (1.05 MeV) and E_{cd} is the cut-off energy (0.55 eV) [14].

Thus, it is possible to obtain the values of the thermal and epithermal neutron flux in each irradiated position.

2.4 Calculation Of Effective Thermal Cross Section of Gold Foil Infinitely Diluted In The Position Of Irradiation And The Corresponding Thermal Neutron Flux using the spectrum calculated by MCNP-4C code.

The saturation activity of the gold foil obtained by irradiation of thermal neutron flux is calculated by equation (4)

$$A^{\infty} = \int_0^{0,55} N_t \cdot \sigma(E) \cdot \Phi(E) dE \quad (4)$$

where N_t is the number of target nuclides foil (gold atoms), $\sigma(E)$ the microscopic cross section as a function of energy and $\Phi(E)$ the neutron flux as function of energy. This expression can only be calculated if the functions $\sigma(E)$ and $\Phi(E)$ are known, although this is not usual.

To make this calculation, the integral equation (4) is replaced by a summation. The energy scale is divided into m energy groups and the differential flux is replaced by its means over these energy intervals. The equation (5) shows that the thermal activity saturation is obtained by summing the total fluxes in m energy intervals multiplied by their cross sections at these intervals.

$$A^{\infty} = N_t \cdot \sum_{j=1}^m \sigma_j \cdot \Phi_j \quad (5)$$

To obtain the values of cross sections in the energy intervals j it is necessary to get the discrete data of cross sections in nuclear libraries and calculate the mean value of cross sections between two consecutive values of energy. Thus, if the value of the cross section for energy $E(j)$ is σ_{E_j} barns and for energy $E(j+1)$ the cross section is $\sigma_{E_{j+1}}$ barns then the mean cross section in the interval of energy E_j and E_{j+1} is given by equation (6)

$$\sigma_j = (\sigma_{E_j} + \sigma_{E_{j+1}}) / 2 \quad (6)$$

The MCNP-4C code allows us to obtain only the relative fluxes Φ_j/Φ_t on the energy intervals. Therefore, to obtain the saturation thermal activity for target nucleus it is necessary to use equation (7)

$$\frac{A^\infty}{N_t} = \Phi_t \left(\sum_{j=1}^m \sigma_j \cdot \Phi_j / \Phi_t \right) \quad (7)$$

Thus, the effective cross section is obtained by equation (8)

$$\sigma_{effective} = \sum_{j=1}^m \sigma_j \cdot \Phi_j / \Phi_t \quad (8)$$

The saturation activity for target nucleus value is obtained experimentally considering experimental corrections, so the total thermal neutron flux can be calculated using equation (9)

$$\Phi_t = \frac{\frac{A^\infty}{N_t}}{\sum_{j=1}^m \sigma_j \cdot \Phi_j / \Phi_t} \quad (9)$$

This methodology results in the mean effective thermal cross section of 85.10 barns for the gold foil at the center of the flux trap configuration number 203.

The graph of Fig. 5 shows the computed spectrum in 640 energy groups calculated by the code MCNP-4C.

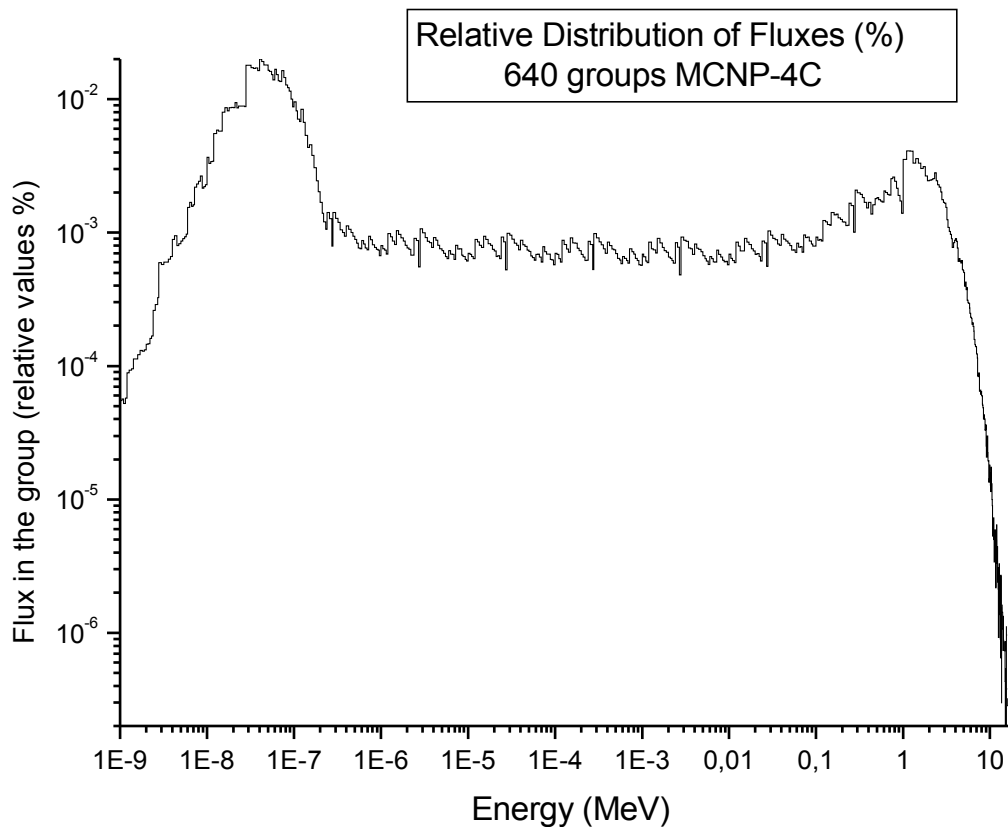


Figure 5. Graphic of the neutron spectrum at the center of Flux Trap configuration 203 calculated in 640 groups of energy by the code MCNP-4C

3. RESULTS OF FLUX TRAPS CONFIGURATIONS

3.1 Configurations of Flux Trap

This work assembled six Flux Trap configurations and table 1 displays the basic data of each configuration. The status column shows whether the configuration has reached criticality. Table 2 compares the results of different Flux Trap configurations showing the thermal and epithermal saturation activities and cadmium ratios. It is possible to see that configuration 203 has the highest ratio of cadmium. All of these irradiations were made to 70.47 watts of reactor power level estimated by nuclear channel 10.

Table 1. Description and status of the Flux Traps by the criterion of criticality

Conf.	Code	Description	Status	Moderator Temperature (°C) ^b	Control Rod Position ^a	
					BC#1	BC#2
195	FT1	FT Square 2X2	CRITICAL	22,55 ± 0,04	58,83	59,27
197	FT2	FT Square 4X4	CRITICAL	22,90 ± 0,19	73,19	73,19
199	FT3	FT Square 6X6	SUBCRITICAL	--	99,62	99,74
201	FT4	FT Losange 6X6	CRITICAL	23,19 ± 0,08	79,15	79,14
202	FT5	FT 6X6 Octagonal	SUBCRITICAL	--	99,63	99,74
203	FT6	FT 6X6 Octagonal Rods in the Edge	CRITICAL	21,89 ± 0,04	90,21	90,22

a. Percentage of control rods removed.

b. Mean of 12 thermocouples arranged within the core.

Table 2. Comparison between the thermal and epithermal saturation activities and the ratios of cadmium of the Flux Traps.

Configuration ^a	Activity thermal saturation ($A_{\text{thermal}}^{\infty}$) (s ⁻¹)	Activity epithermal saturation ($A_{\text{epithermal}}^{\infty}$) (s ⁻¹)	Cadmium Ratio (R_{cd})
203	2,70967. 10 ⁵ ± 2,38 %	7,39940. 10 ⁴ ± 2,38%	4,66 ± 3,37 %
201	2,81346. 10 ⁵ ± 2,38 %	8,84747. 10 ⁴ ± 2,38%	4,18 ± 3,36 %
197	2,97247. 10 ⁵ ± 2,38 %	1,01211. 10 ⁵ ± 2,38 %	3,94 ± 3,37 %
195	2,35795 . 10 ⁵ ± 2,38 %	1,25184 . 10 ⁵ ± 2,38 %	2,88 ± 3,37%

a. All of these irradiations were operated in the same reactor power level (70.47 watts).

Table 3 shows the thermal and epithermal fluxes and the ratio between the fluxes of the Neutron Flux Trap configurations obtained using the data of table 2. Configuration 203 has the highest thermal neutron flux. We can see in table 2 that values of thermal flux in configurations 203, 201 and 197 are very close despite the increase in cross-section Flux Trap. Thus, the cross section of Flux Trap has an optimum dimension beyond which no increase of the thermal neutron flux occurs. The higher the cross-sectional dimension of the Flux Trap, the lower the epithermal neutron flux at the center of the Neutron Flux Trap will be.

Table 3 - Comparison between the thermal and epithermal neutrons fluxes of different core configurations with Neutron Flux Traps.

Configuration ^a	Thermal Flux (neutrons/ cm ² s)	Epithermal Flux (neutrons/cm ² s)	Ratios between fluxes
203	2.8945 10 ⁹ ± 3,44 %	8.8458 10 ⁸ ± 4,12 %	3.27 ± 5,37 %
201	2.8544 10 ⁹ ± 3,89 %	1.0732 10 ⁹ ± 4,12 %	2.66 ± 5,66 %
197	2.8861 10 ⁹ ± 4,06 %	1.2277 10 ⁹ ± 4,12 %	2.35 ± 5,79 %
195	1.5340 10 ⁹ ± 5,93%	1.5151 10 ⁹ ± 4,12%	1.01 ± 7,22%

a. Power Reactor level of the 70.47 watts (Nuclear Channel 10).

3.2 Comparison Between The Standard Reactor Core Configuration And Core Configuration Number 203

Table 4 shows the comparison between the standard configuration of 28x26 rods and configuration 203, which is considered the most efficient Neutron Flux Trap configuration. In this Table is possible to compare of the variation of thermal and epithermal fluxes at the central position of the reactor core that correspond to the central position of the Neutron Flux Trap (axial position 346.00 mm and radial position 222.40 mm).

It is very interesting to see that the Neutron Flux Trap increases the thermal flux in 337.0% value at the central position of the reactor core. In this position the neutron flux at 106 watts power level is (1.004 10⁹ ± 7,05% neutron/cm².s) [12] and to normalize the power level we must reduce this value to the power level of 67.89 watts (channel 10) to correspond to the same power level that is irradiated the Au-Al foil in the Neutron Flux Trap configuration 203 in this comparison. The thermal neutron flux normalized by the same reactor power level is then equal to (6.4303 10⁸ ± 7.05% neutron/cm².s) at the central position of the standard rectangular configuration core.

Table 4 - Comparison between the standard configuration and configuration 203 at the central position of the Flux-Trap (FT) that shows the variation of thermal and epithermal neutron fluxes

Energy (MeV)	Nêutron integral Flux – Configuration 203 ^b (n / cm ² s)	Neutron integral Flux Standard Configuration ^{a,b} (n / cm ² s)[2]	Ratio between the Fluxes
Φ thermal flux < 0,55 10 ⁻⁶	2.811 10 ⁹ ± 1,42 %	6.4282 10 ⁸ ± 7,05 %	4.37 ± 7,19 %
Φ epithermal flux 0,55 10 ⁻⁶ at 1,05	9.4117 10 ⁸ ± 5,54 %	1.189 10 ⁹ ± 1,44 %	0.79 ± 5,72%
Φ Total	3.7522 10 ⁹ ± 1,75%	1.832 10 ⁹ ± 8,97 %	2.05 ± 9,13%

a Array of 28x26 fuel rods (680 fuel rods, 24 control and 24 safety).

b The irradiation reactor power level is 67.89 watts .

3.3 Spatial Flux Distribution

The Fig. 5 shows the axial spatial distribution of thermal and epithermal neutron flux inside the reactor core in the configuration number 203 at power level 67.89 watt.

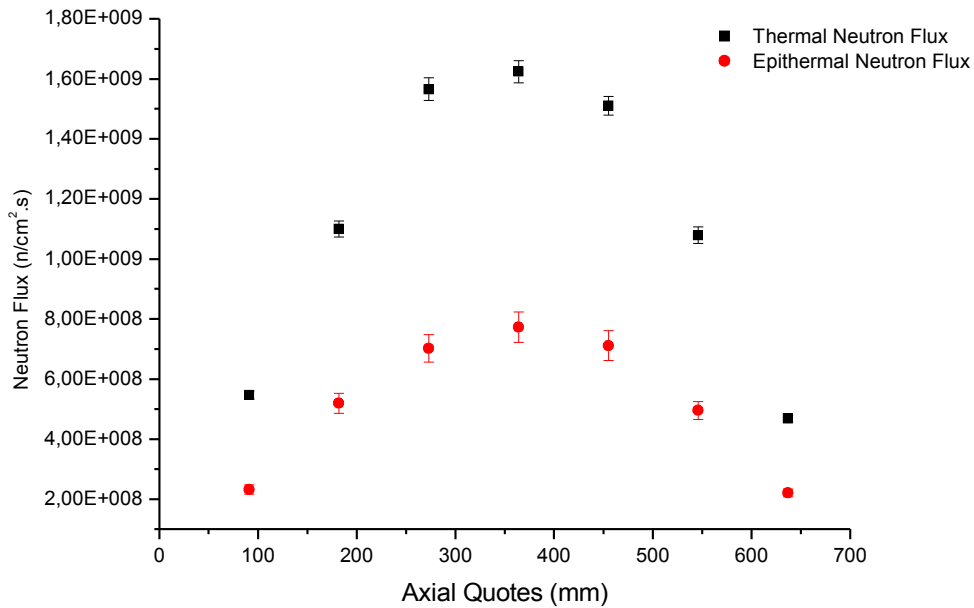


Figure 5. Thermal and Epithermal neutron flux in the Axial quotes.

The Fig. 6 shows the radial spatial distribution of thermal and epithermal neutron flux inside the reactor core in the configuration number 203 at power level 67.89 watt .

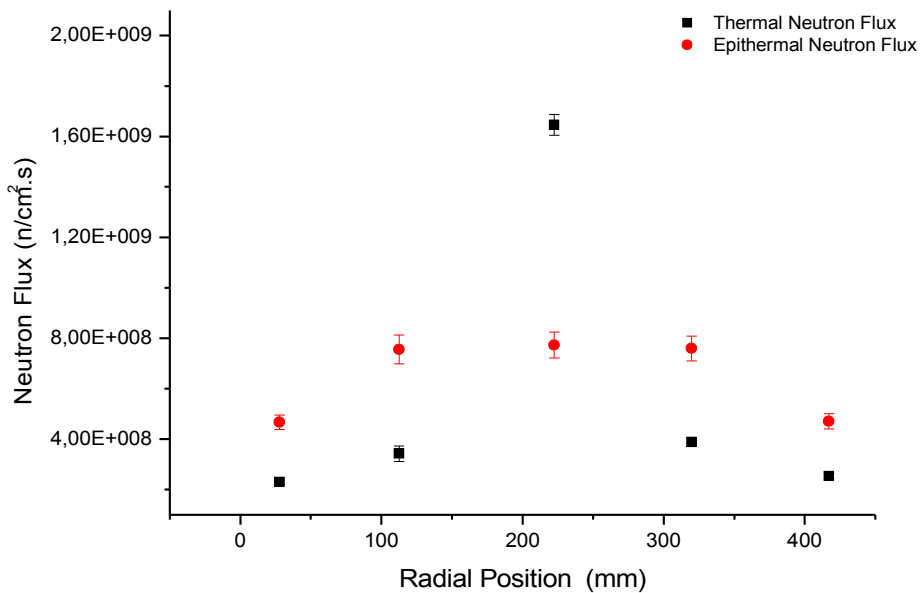


Figure 6. Thermal and Epithermal neutron flux in Radial Quotes .

The next tables show the absolute thermal and epithermal neutron flux obtained to each irradiation positions at axial and radial quotes at the IPEN/MB-01 reactor core with the neutron flux trap.

Table 5 -Thermal and Epithermal neutrons Fluxes in configuration 203 in radial positions reactor operating at 67,89 watts power level (channel 10)

Radial Position (mm)	Thermal Flux (neutron/ cm ² . s ¹)	Epithermal Flux (neutron/ cm ² . s ¹)
27,75 ^b	2.852 10 ⁸ ± 4.29%	5.6847 10 ⁸ ± 5.23%
125,075 ^c	4.291 10 ⁸ ± 8.00%	9.1979 10 ⁸ ± 6.15%
222,4 ^a	2.811 10 ⁹ ± 1.42%	9.4117 10 ⁸ ± 5,55%
319,725 ^c	4.870 10 ⁸ ± 4.73%	9.2500 10 ⁸ ± 5.47%
417,05 ^b	3.149 10 ⁸ ±4.61%	5.7303 10 ⁸ ± 5,47%

a- Activation cross section value to Gold activation Foil: 85.10 barns

b- Activation cross section value to Gold activation Foil: 71.966 barns

c- Activation cross section value to Gold activation Foil: 71. 121 barns

Table 6. Thermal and Epithermal neutrons Fluxes in configuration 203 in axial positions reactor operating at 67,89 watts power level (channel 10)

Axial Positions (mm)	Thermal Flux (neutron/ cm ² . s ¹)	Epithermal Flux (neutron/ cm ² . s ¹)
91 ^a	9.459 10 ⁸ ± 1.57%	2.8250 10 ⁸ ± 5.47%
182 ^a	1.904 10 ⁹ ± 1.49%	6.3245 10 ⁸ ± 5.47%
273 ^a	2.710 10 ⁹ ± 1.53%	8,5529 10 ⁸ ± 5.47%
364 ^a	2.811 10 ⁹ ± 1.42%	9.4117 10 ⁸ ± 5,55%
455 ^a	2.615 10 ⁹ ± 1.3%	8.6580 10 ⁸ ± 5.81%
546 ^a	1.868 10 ⁹ ± 1.62%	6.0302 10 ⁸ ± 5.22%
637 ^a	8.111 10 ⁸ ± 1.6%	2.6869 10 ⁸ ± 5.07%

a- Activation cross section value to Gold activation Foil: 85.10 barns

4. CONCLUSIONS

This work showed that the assembly of Neutron Flux Traps in nuclear reactors can be an alternative to increase the thermal neutron flux in the region of irradiation. For this analysis to be more accurate it is necessary to insert samples at the center of the Neutron Flux Trap and check if the increase of the thermal neutron flux generates a proportional increase in the nuclear reaction rates at the samples irradiated. The thermal neutron flux increased 337% at the center of the Neutron Flux Trap (Configuration number 203) compared to the standard configuration 28x26 rods with a significant decrease in the epithermal neutron flux. To obtain the spatial distribution of thermal flux across the radial extent of the neutron flux trap, activation detectors in the form of wires can be used. As a suggestion for further work flux traps could be assembled at the edges of the reactor core exploring the reflective effect of the moderator in these regions and the fact that at these positions the removal of fuel elements generates a lower loss of reactivity.

ACKNOWLEDGMENTS

The authors are grateful to reactor staff operators of the IPEN/MB-01 reactor, Mr. Rogério Jerez, Cesar Luiz Veneziani, Rinaldo Fuga, Marco A. Sabo and Reginaldo Gilioli.

REFERENCES

1. H. Khalafi, M. Gharib, "Optimization of ^{60}Co production using neutron flux trap in the Tehran research reactor." ,*Annals of Nuclear Energy*, **32**, pp. 331-341 (2005).
2. L. B. Gonçalves, "Calibração dos canais nucleares do Reator IPEN/MB-01, obtida a partir da Medida da Distribuição Espacial do Fluxo de Nêutrons Térmicos no Núcleo do Reator Através da Irradiação de Folhas de Ouro Infinitamente Diluídas.", Dissertação de mestrado, IPEN (2008).
3. G. F. Knoll, *Radiation detection and measurement*, John Wiley & Sons (1989).
4. T. Bitelli, *Física e Dosimetria das Radiações 2ª Edição*, Ed. Atheneu (2006).
5. D.D. Glower, *Experimental reactor analysis and radiation measurement*, McGraw-Hill, New York (1965).
6. International Atomic Energy Agency. , "Nêutron Fluence Measurent", Vienna ,Technical Reports Series n° 107., Vienna (1970).
7. N. Tsoulfanidis, D.R. Edwards, L. Kao, F.Yin, "Neutron fluence and threshold foil reaction rates in PWRs", *Trans. Am. Nucl. Soc.*, **45**, pp.592-3 (1983).
8. Library ENDF/B-VII.0, <http://www.nds.iaea.org/exfor/endl.htm>
9. J.F. Briemeister, *MCNP: A General Monte Carlo N-Particle Transport Code (Version - 4C)*. Los Alamos National Laboratory, LA-13709-M (2000).
10. C.D. Harmon, R.D.Busch, J.F. Briesmeister, R.A. Forster, *Criticality calculations with MCNP: A Primer*, Los Alamos National Laboratory, LA-12827-M Manual (1994).
11. F.R. Martins, "Medida de Parâmetros Nucleares de um Reator de Potência Zero Aplicando a Técnica de Análise de Ruídos." , IPEN, Dissertação de mestrado, (1992).
12. R.Diniz,, Personal communication . IPEN, (2011)
13. L.E.C.Mura. "Caracterização dos Campos Neutrônicos Obtidos por Meio de Armadilhas de Nêutrons no Interior do Núcleo do Reator IPEN/MB-01", IPEN-CNEN/SP, São Paulo (2011).
14. F. Bench, "Flux Depression and The Absolute Measurements of the Thermal Neutron Flux Density" , *Atomkernergie*, **25 (4)** , pp. 257-263 (1975).